Acta Crystallographica Section A
Foundations of Crystallography
ISSN 0108-7673

Received 24 February 2003
Accepted 9 October 2003

Ultra-high-angle double-crystal X-ray diffractometry (U-HADOX) for determining a change in the lattice spacing: experiment

Koji Munakata and Atsushi Okazaki*

Department of Physics, Kyushu University, Fukuoka 812-8581, Japan. Correspondence e-mail: hadx6scp@mbox.nc.kyushu-u.ac.jp

An experiment is reported on ultra-high-angle double-crystal X-ray diffractometry (U-HADOX) at the Bragg angle θ up to 89.5°, coupled with white X-rays from a conventional source. It is shown that the Bragg-peak shift associated with a change in the lattice spacing increases in proportion to $\tan\theta$ as predicted; the relative accuracy of a change in the spacing to 10^{-8} is attained. The performance is demonstrated for the determination of the linear thermal-expansion coefficient α of silicon and strontium titanate $SrTiO_3$, a value with four significant figures being determined with the data in a temperature range narrower than 1 K; the value of α for silicon $(2.621 \pm 0.003) \times 10^{-6}\,K^{-1}$ at 300.4 K is compared with those in the literature based on experiments using the Bond method of X-ray diffraction and macroscopic thermal expansion. The advantages and characteristics of U-HADOX including the coupling with synchrotron X-rays are discussed.

1. Introduction

For determining the temperature dependence of the lattice spacing, high-angle double-crystal X-ray diffractometry (HADOX) (Okazaki & Ohama, 1979) is appropriate in general; the accuracy of this method is 10^{-6}–10^{-7} depending on the crystal quality. Owing to low intensities of white X-rays from conventional sources, most HADOX experiments have been carried out with characteristic X-rays at Bragg angles around 80° at the expense of accuracy. In the circumstances where white X-rays of synchrotron radiation are easily available to many crystallographers, Okazaki & Soejima (2001) (referred to as OS in the following) have proposed to extend the Bragg-angle range to ultimately high angles in order to utilize fully the inherent advantages. The characteristics have been examined theoretically and found to be more advantageous than those of HADOX at moderately high angles; the method is called ultra-high-angle double-crystal X-ray diffractometry (U-HADOX).

The purpose of the present paper is to examine, by experiment with a conventional X-ray source, the characteristics and performance of U-HADOX, and to show an example, for silicon, of the determination of the temperature derivative of the lattice spacing, *i.e.* the linear thermal-expansion coefficient. Data are also given in a lower angle range (80–89°) to trace the variation of the performance. Subsidiary experimental data on $SrTiO_3$ are given to show the validity of this method also for crystals of ordinary quality, being less perfect than silicon.

2. Fundamentals

Through HADOX, one can attain high sensitivity for a change in the lattice spacing by high-angle diffractometry, and obtain high resolution by the double-crystal arrangement. The experimental arrangement shown in Fig. 1(*a*) is called the S–A arrangement, which is suitable for measurements with white X-rays as incident beams, and used in the present experiment. Here, S and A respectively stand for specimen and analyser. (The monochromator–specimen arrangement is called the M–S arrangement.)

For the S–A arrangement, Bragg's law can be given by

$$d_S \sin\theta_S = d_A \sin\theta_A, \qquad (1)$$

where d and θ respectively denote the lattice spacing and the Bragg angle. The equation results from Bragg's law for the first and second crystals for a common wavelength. In the experiment, θ_S and d_A are kept constant. Therefore, a change in d_S, *i.e.* a change in the lattice spacing of the specimen, can be determined from a change in θ_A of the second crystal. The requirement $d_S \sim d_A$ is essential for the dispersion-free condition. The thermal-expansion coefficient of the specimen crystal can be determined over a wide temperature range if the analyser temperature is adjusted according to the specimen temperature.

3. Experimental

The apparatus used in the present experiment had a structure that is similar, but with some modifications, to that used in

previous HADOX experiments, the diffractometer plane being horizontal. Each of the two goniometers had at least two rotation axes (ω and χ); the ω axes of the two goniometers were vertical, the distance between them being 1.050 m. The minimum ω steps of the first and second goniometers were 2×10^{-4} and 1.4×10^{-6} degrees, respectively. The χ axis was used for tilting the crystal for the alignment. The total length of the beam path was about 3 m, a part of which was evacuated to reduce the effect of absorption by air. When the detector was placed at the position shown in Fig. 3 of OS, the observation of diffraction was not practicable owing to the high background. The detector was thus placed as schematically shown in Fig. 1(a); for catching the diffracted beams at highest angles, the front face of the detector was not normal but almost parallel to the beams. The upper limits of θ for a scintillation counter and a germanium detector were 89.5 and 86°, respectively, depending on the size and structure of the equipment; step scanning of the detector was not necessary. The rotating-anode X-ray generator was operated in a fine-focus mode at 50 kV and 40 mA. A gold-plated anode was used for emitting white X-rays; a thin copper film was further plated on part of the gold surface, as Cu $K\alpha$ X-rays were useful for the crystal alignment.

Specimen and analyser crystals were prepared from a high-purity dislocation-free floating-zone (FZ) crystal, with impurity concentrations of phosphorus, boron and oxygen less than 5×10^{18}, 1×10^{19} and 1×10^{22} atoms m^{-3}, respectively. The shape was, as shown in Fig. 1(b), a plate $9 \times 6 \times 2$ mm in size; the largest face, where the incident beam impinged, was parallel to (111). The bottom of each crystal was glued to the holder made of copper; it was important to make the cuts shown in Fig. 1(b) to keep the crystal area being examined stress free. Inside the vacuum container with an X-ray window of Be film, the crystal was covered with the cap of the holder with a Be window and with doubled thermal-radiation shields with aluminized Mylar windows; the assembly was mounted on a closed-cycle cryostat used as a thermostat in the present experiment, and finally mounted on a relevant goniometer. The unit shown in Fig. 1(b) was thermally disconnected from the main part of the cryostat.

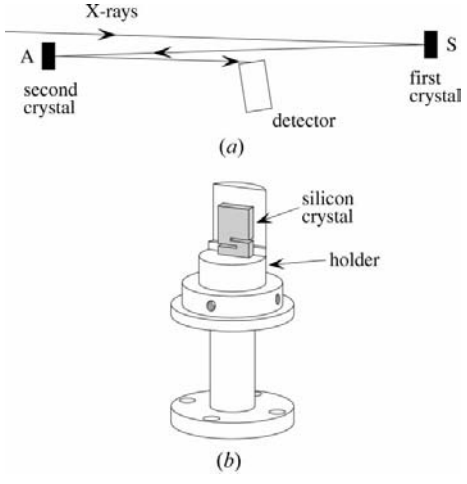

Figure 1
(a) The experimental arrangement of U-HADOX (the S–A arrangement); the deviation from $\theta = 90°$ is exaggerated. (b) Silicon crystal with two cuts and the holder.

The temperature control procedure was as follows: a silicon diode attached to the holder was used as a sensor for the temperature controller (Lake Shore/DRC-91CA), the minimum setting of the temperature step being 10 mK. Two sets of Cu–constantan thermocouples attached to the crystal and the holder were used as sensors to monitor the temperature stability through a digital voltmeter with a minimum interval of 10 nV, corresponding to the temperature variation of 0.25 mK around 300 K. No temperature difference was observed between the two positions. During a series of measurements over two days, the temperature fluctuation indicated by the voltmeter was less than ±1 mK. For each crystal, the same type of sensor and controller was used. In the present experiment, we do not need to be very accurate with the absolute value of the temperature because our interest is in the amount of temperature variation. Temperature values given in the following are those indicated on the voltmeter.

In a HADOX experiment coupled with white X-rays, we need values of θ of the diffraction observed at the first crystal for determining the value of the linear thermal-expansion coefficient α. The θ value can be determined by measuring either the separation between the incident and diffracted beams at a known distance from the crystal or the difference between the two angular positions of the Bond-method measurement (Bond, 1960). In the condition of the present experiment, the latter has been chosen as a more accurate procedure.

The crystal alignment was carried out to make the scattering vector parallel to the diffractometer plane, and to determine, simultaneously, the angular position of $\theta = 90°$ of the first goniometer. First, each crystal on the relevant goniometers was successively brought into the position on the line of the incident beam from the collimator. By choosing an appropriate diffraction, for example 444 of silicon for Cu $K\alpha$, the χ position of the goniometer that gave the smallest nominal θ value was determined; the minimum step of the χ arm was 0.002°. By this, the possible tilt error mentioned in OS was made insignificant. Second, by applying the Bond method on each side of the incident beam, the position of $\theta = 90°$ of the first goniometer was determined. The importance of the determination of this position will be discussed later in the second paragraph of §6. Then, the second goniometer was shifted to the position of the HADOX measurement to set up and adjust the whole diffractometer. For the second crystal, the θ value was evident from the relation $\theta_A = \theta_S$ when the two crystals were at the same temperature. It was finally confirmed that the height of the X-ray beams were kept constant within ±0.1 mm over the whole path to the detector. Therefore, the magnitude of the deviation from the horizontal plane was estimated to be less than 0.01°; the error in θ will not be serious for θ up to 89.5°.

The present experiment thus consists of two parts: one using the Bond method with characteristic X-rays, and the other using HADOX with white X-rays. In either experiment, the

diffraction intensity at a specific θ value is measured as a function of ω, the angular position of the specimen or analyser. For the Bond-method experiment, it is not necessary to choose the diffraction at highest angles. A more serious requirement is that the HADOX experiment should follow the Bond-method experiment, and be completed without introducing a change in the environment of the electron gun of the X-ray generator. Exchanging one anode with another during a series of experiments, for instance, may give rise to a difference between the θ value determined by the Bond method and the actual θ value to be assigned in HADOX.

HADOX measurements were made with one crystal at a constant temperature and the other at temperatures around it, the range of the temperature variation being limited by the matching condition of the lattice spacing (*cf.* OS). By the symmetry of the arrangement, one can regard either of the crystals as the specimen.

4. Specifications of U-HADOX

4.1. Peak shift

The main factor that determines the accuracy of HADOX is the sensitivity $\Delta\theta_A/\Delta d_S$, which is proportional to $\tan\theta$, which divergently increases when θ approaches 90°; the measurement at highest angles is therefore advantageous. The value of $\tan\theta$ increases by a factor of 20 for the increase of θ from 80.0 to 89.5°.

Fig. 2 shows the preliminary results of the peak shift of the *hhh* diffraction of silicon at $\theta = 79.0$, 89.0 and 89.5° in a temperature range 2 K around 301 K. Error bars are not shown because they are smaller than the size of the data points. Observed peaks consist of a series of the *hhh* components, excluding those prohibited by the symmetry. The wavelength range corresponding to $\theta = 79.0$–89.5° is rather narrow, being 0.1539–0.1568 nm for $h = 4$, for example. For the temperature range shown in the figure, the change in d_S is proportional to the change in temperature. The results show that the values of $\Delta\theta_A/\Delta d_S = \Delta\omega_A/\Delta d_S$ at the three θ values are in the ratio 0.9 : 10 : 20, which is in good agreement with the ratio of $\tan\theta$. The sensitivity can further be enhanced by a factor of ten at $\theta = 89.95°$, theoretically at least.

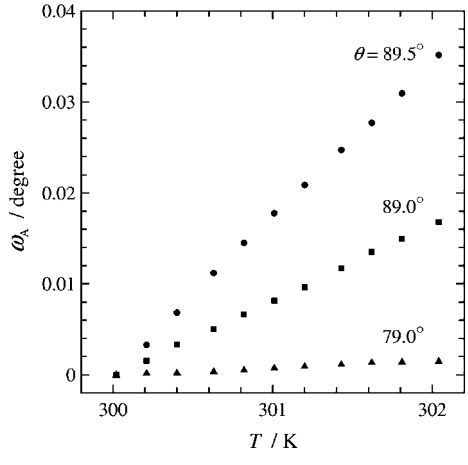

Figure 2
Peak shifts of *hhh* of silicon at $\theta = 79.0$, 89.0 and 89.5° for a temperature variation of 2 K around 301 K.

4.2. Peak width

Before discussing the profile of the rocking curve, we need to check the energy spectrum; Fig. 3 is an example of such spectra measured with an energy-sensitive germanium detector at the highest accessible angle $\theta = 86°$. The figure shows that the *hhh* peak observed with a scintillation counter consists of a series of components with $h = 3$–12; the relative intensities of them mainly depend on the crystal structure factor $F(hhh)$ and the spectrum of incident X-rays. Fig. 4 shows the rocking curves of the *hhh* reflection of silicon measured with a scintillation counter at $\theta = 89.5°$; the two crystals were at 300 K. In Fig. 4(*a*), the dashed curves represent two components, broad and narrow, both Lorentzian, the full curve being the sum of them; in Fig. 4(*b*), the broader

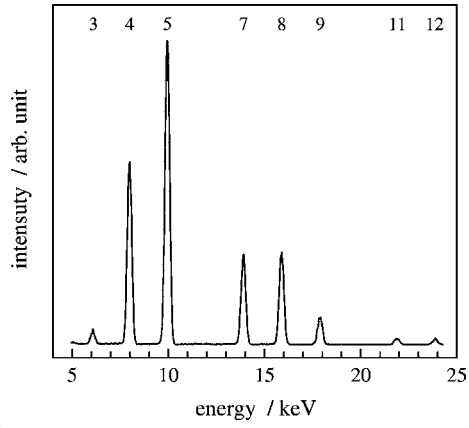

Figure 3
Spectrum of *hhh* of silicon at $\theta = 86°$ measured by HADOX with a germanium detector. Numerical figures at the top are h values of *hhh* for relevant peaks.

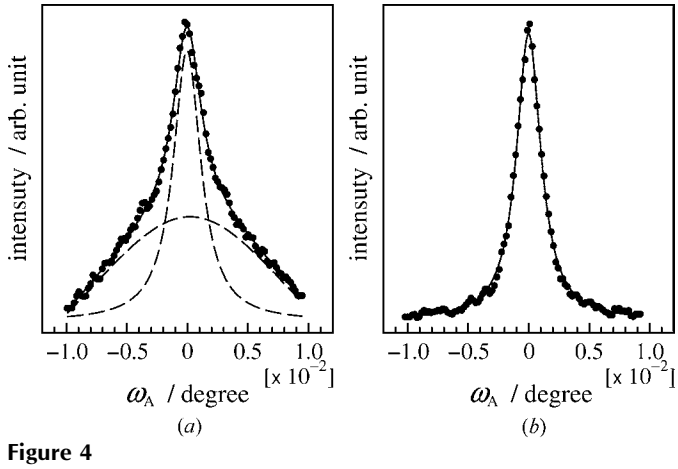

Figure 4
Peak profiles of *hhh* of silicon observed by U-HADOX at $\theta = 89.5°$ and 300 K. In (*a*), the dashed curves represent two components, broad and narrow; the full curve is the sum of them. For both the components, a fit is made with a Lorentzian. In (*b*), the broader component is discriminated.

component is filtered out by discriminating a lower energy part of the output of the detector.

In Fig. 5, the full width at half-maximum (FWHM) of the rocking curve is traced as a function of θ: Figs. 5(*a*) and (*b*) are respectively those for the narrower and broader components mentioned above, and Fig. 5(*c*), for comparison, that measured by the Bond method for the 444 diffraction of one of the crystals used in the HADOX experiment mentioned above. In the Bond-method experiment, a quadruple-crystal monochromator (QCM) (Bartels, 1983; Lu *et al.*, 1995) is coupled. The difference between the magnitudes of the FWHM observed by the two methods is striking. The narrower component of the HADOX peak has FWHM less than 1/100 of that observed by the Bond method; this is due to a dispersion-free double-crystal arrangement. According to the dynamical theory of X-ray diffraction, all the FWHM's shown here can be expressed by $A + B(1 + |\cos 2\theta|)/\sin 2\theta$ or $A + B\tan\theta$.

The dynamical theory also shows that the peak width of the rocking curve at a given θ is proportional to $|F(hkl)| \times \lambda^2$, where λ denotes the X-ray wavelength for relevant *hkl*'s. Both $|F(hkl)|$ and λ decrease with increasing *hkl*. The peak width, therefore, rapidly decreases with increasing *hkl*. The peak profile observed with a scintillation counter is a superposition of the profiles of relevant *hkl*'s, each being Lorentzian. After fitting, it is found that the main contributions to the peak profile shown in Fig. 4(*a*) are those from 444 and 555 in the broader component, and 777 and 888 in the narrower one; this is consistent with the spectrum shown in Fig. 3. By discriminating the broader component, we can attain higher precision in determining the peak position, reducing both the FWHM and the background fluctuation. In Table 1, theoretical values of the peak width (the Darwin width) of silicon at $\theta = 89.5^\circ$ are given for various *h* values of *hhh*, showing how rapidly the width decreases with increasing *h*. The experimental value of the width (FWHM) of each *hhh* determined by the fit mentioned above is consistent with that given in the table. With the goniometer with a minimum step of 1.4×10^{-6} degrees, one can follow the profile of the rocking curve of the *hhh* peaks with *h* up to 13 or more.

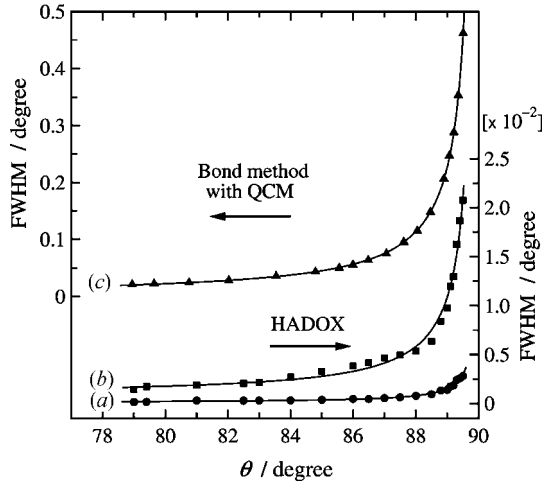

Figure 5
Peak widths (FWHM) of *hhh* of silicon as functions of θ observed in the HADOX experiment and in the Bond-method experiment coupled with a QCM: (*a*) and (*b*) for the narrower ($h \geq 7$) and broader ($h \leq 5$) components observed by HADOX, respectively, and (*c*) for 444 by the Bond method. Curves are functions $A + B(1 + |\cos 2\theta|)/\sin 2\theta$ fitted to the data.

Table 1
Theoretical values of the Darwin width of silicon at $\theta = 89.5^\circ$ for various *h* values of *hhh*'s, together with relevant X-ray energy and penetration depth, defined by $\sin\theta/2\mu$, μ being the linear absorption coefficient.

h	Darwin width (10^{-2} degrees)	Energy of diffracted X-rays (keV)	Penetration depth for silicon (mm)
3	5.24	5.9	0.015
4	2.95	7.9	0.033
5	0.90	9.9	0.064
7	0.21	13.8	0.173
8	0.16	15.8	0.256
9	0.06	17.8	0.361
11	0.021	21.7	0.648
12	0.018	23.7	0.833
13	0.007	25.7	1.040

5. Performance in determining $\alpha(T)$

As a demonstration of the application of U-HADOX, the temperature dependence of the linear thermal-expansion coefficient $\alpha(T)$ has been determined for silicon because the most accurate reference data were available. Measurements have been made on the peak shift of *hhh* ($h \geq 7$) at $\theta = 89.5^\circ$ in the temperature range 300–320 K. A series of measurements of the crystal alignment and of U-HADOX were carried out with X-rays from the Au anode previously mentioned by keeping the operating condition of the generator constant.

Fig. 6 shows the temperature dependence of the lattice constant $a(T)$ of silicon determined in the range 300.000–300.800 K at intervals of 0.200 K, with the temperature of the

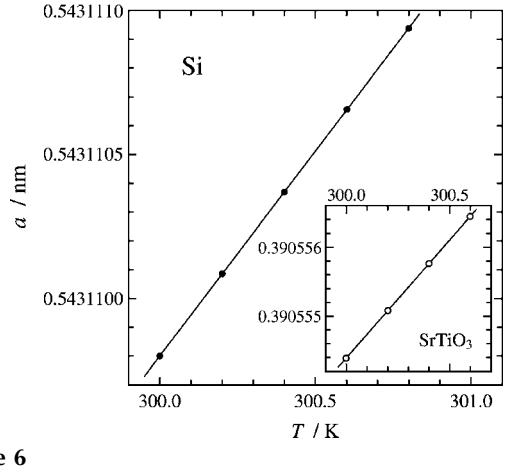

Figure 6
Temperature dependence of the lattice constant of silicon determined from the peak shift of *hhh*, and of $SrTiO_3$ from *hh*0 given in the inset. Both the data sets are obtained at $\theta = 89.5^\circ$; error bars are not given because they are smaller than the size of the data points.

first crystal fixed at 300.000 K; by the fit of the peak profile, the relative precision of the lattice spacing is estimated to be 3×10^{-9}. The values of the lattice constant are normalized to 0.5431098 nm at 300.0 K on the basis of the data given by Okada & Tokumaru (1984). The absolute value of the lattice constant is not very important; in fact, we need only the top four or five figures of the lattice constant for determining $\alpha(T)$. The line in the figure is a least-squares fit of the linear temperature dependence, corresponding to $\alpha = (2.621 \pm 0.003) \times 10^{-6}$ K^{-1} representing the value at 300.4 K, the arithmetic mean of the five temperatures where the measurements were made. It should be noted that the value of α will be affected neither by a possible systematic error in the lattice constant nor by a choice of the standard point of the temperature in a relevant range, and that there is no normalization in determining α. The precision indicates that one can detect the effect of temperature shift by a few mK on the lattice spacing. The data of five points in the figure were collected in 2 days. As observed from FWHMs of the peaks shown in Fig. 7, the effect of the mismatch between the lattice spacings of the two crystals around 300 K, at this θ value, is not significant for a temperature difference less than 1 K, but is significant for larger differences. The inset shows that one can detect a peak shift for a temperature change of a few mK, being consistent with the previous description. In comparison with U-HADOX, the Bond-method X-ray diffraction is less accurate: the results given by Batchelder & Simons (1964) and Okada & Tokumaru (1984) are based on the measurements at temperature intervals several tens of K, and are (2.64 ± 0.04) and $(2.58 \pm 0.05) \times 10^{-6}$ K^{-1}, respectively, at 300 K.

Measurements have been extended to a few more temperatures; the values of α determined in a similar way are plotted in Fig. 8. The temperature of the reference crystal was varied according to that of the specimen crystal, and kept at the lowest temperature of each series of measurements at five temperatures. Also shown in Fig. 8 are the data given by Lyon *et al.* (1977) and by Norton *et al.* (1976). It is remarkable that the three data sets of α with highest accuracy are in very good agreement with each other, although the experimental techniques are all different. Lyon *et al.* (1977) and Norton *et al.* (1976) respectively used a three-terminal capacitance method with a polycrystal 100 mm in length, and a Fabry–Perot interferometer with a single-crystal 100 mm in length, the measurements being made at temperature intervals of 5 and 1.9 K, respectively; the points in the figure represent α values at the respective average temperature for each interval, while each point for U-HADOX is based on five data points in a range of 0.8 K as shown in Fig. 6. This means that U-HADOX surpasses the level of accuracy of the macroscopic thermal-expansion experiments that have been regarded as the highest. More recent data by Bergamin *et al.* (1997) based on combined X-ray/optical interferometry give $\alpha = (2.581 \pm 0.002) \times 10^{-6}$ K^{-1} at 295.5 K. This is in quantitative agreement with those in Fig. 8. As mentioned in OS, U-HADOX is more general and gives information on the atomic scale. It is therefore obvious that U-HADOX will be the best method to determine the thermal expansivity, as far as crystalline materials are concerned provided that the intensity at high angles can be measured; in other words, U-HADOX will not be applicable to general organic crystals. All the methods mentioned above are not applicable to measurements at very high temperatures. Watanabe *et al.* (2002) developed a dilatometer based on an optical heterodyne interferometry that is applicable at temperatures as high as 2000 K.

It is confirmed that U-HADOX is also applicable to ordinary imperfect crystals with FWHM about one order of magnitude larger than that of silicon. For a couple of Verneuil crystals of $SrTiO_3$, measurements similar to those mentioned

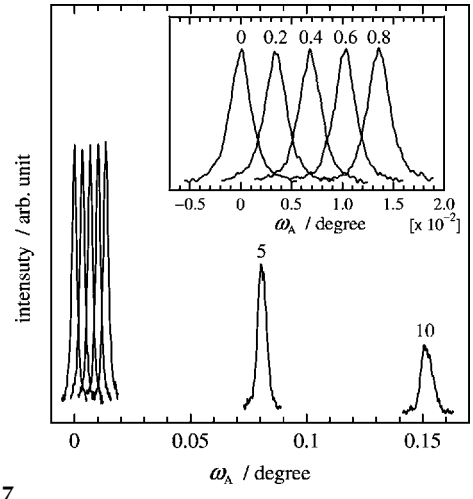

Figure 7
Effect of the mismatch between the lattice spacings of the two crystals on the peak profile and shift. Numerical figures above the peaks indicate the temperature difference in K between the crystals. The inset indicates that the effect on the FWHM is negligible for a temperature change within 1 K. The reference crystal is kept at 300.000 K.

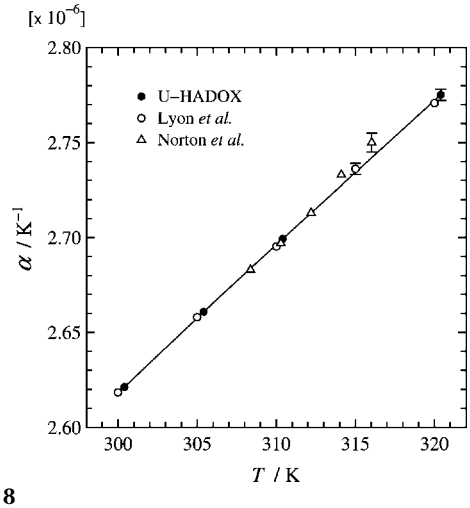

Figure 8
Temperature dependence of the linear thermal-expansion coefficient α of silicon around 310 K determined by U-HADOX compared with those based on the macroscopic experiments by Lyon *et al.* (1977) and Norton *et al.* (1976). For the data of each experiment, the error bar is given at only one temperature, as the size is constant over the temperature range in the figure. The line, a guide for the eye, is drawn through the data points of U-HADOX.

above have been made for $hh0$ at $\theta = 89.5^\circ$. From the data shown in the inset of Fig. 6, we find $\alpha = (8.753 \pm 0.006) \times 10^{-6}\ \mathrm{K}^{-1}$ at 300.3 K. The lattice constant values are normalized to 0.39053 nm at 293 K, based on the data given by Bednorz & Scheel (1977). The old data $\alpha = 8.9 \times 10^{-6}\ \mathrm{K}^{-1}$ in the range 200–300 K (Okazaki & Kawaminami, 1974) is consistent with the new data. It should be pointed out that the relative precisions of α for Si and $SrTiO_3$ attained by U-HADOX are comparable even though the crystalline quality is quite different; *i.e.* the value of the FWHM for $SrTiO_3$ $hh0$ ($h \geq 5$) was about eleven times as large as that of Si mentioned above. It can be concluded that the drawback because the larger FWHM is cancelled out by a larger value of α, which brings about a larger peak shift; the advantages expected from the smaller FWHM of silicon is suppressed by a limited precision of temperature control (1 mK).

Another point to be mentioned is that one can obtain information, distinguishing hhh's or $hh0$'s with different h, in the regions with different depths from the surface. For example, as shown in Table 1, the penetration depth for X-rays relevant to hhh's of silicon is in the range 0.015–1.04 mm for $h = 3$–13. Here we define the penetration depth $(\sin\theta/2)x$ by $\exp(-\mu x) = 1/e$, μ being the linear absorption coefficient. If both the coupled crystals are perfect, all the hhh's appear at the same ω position. In fact, in the present experiment on silicon, they appeared at the same ω position within the experimental error. If there is inhomogeneity in the lattice spacing as a function of the depth, one may find the intensity distribution of some hhh components at ω positions different from those of others, although the analysis of the data might not be straightforward. Moreover, such inhomogeneity may appear when the temperature varies in special crystals; this can also be traced by U-HADOX. Using synchrotron X-rays, we can measure diffraction in a region of higher energies, the corresponding penetration depth possibly reaching 10 mm. This suggests an application of this technique to the semiconductor industry and other fields.

6. Discussion

A typical example of the speciality of U-HADOX is given in Fig. 9; the changes in the peak position and width (FWHM) are respectively shown in Figs. 9(*a*) and (*b*) for silicon at $\theta = 79.3$ and 89.5° as functions of the tilt angle of the second crystal. The tilt introduces a tilt of the reciprocal lattice relative to the Ewald sphere; this brings about a change in nominal θ values as shown in Fig. 9(*a*), and simultaneously an increase of FWHM, shown in Fig. 9(*b*), owing to a change in matching with the first crystal. At $\theta = 89.5^\circ$, the effect of the tilt on the FWHM is so remarkable that the effect may be used for monitoring accidental failure in the crystal alignment during the experiment. It should be added that the dominant contribution of the peak observed at $\theta = 89.5^\circ$ is due to 777 and 888 as previously mentioned, while that at $\theta = 79.3^\circ$ is due to 444 matched with Cu $K\alpha_1$ radiation. The situation that the minimum FWHM's of these are comparable will be seen in the curves (*a*) and (*b*) in Fig. 5. Fig. 9 also suggests that for the experiment at $\theta = 89.95^\circ$ we need more precise alignment, and that at $\theta \sim 90^\circ$ the χ and ω scans are indistinguishable.

A systematic error that was not mentioned in OS has been recognized during the present experiment. Assuming that the scale of θ is correct, we examine here the error in α contributed from the error in the goniometer angular position of $\theta = 90^\circ$. By a numerical calculation for 555 of silicon, we find that an error of 0.001° in θ will result in the error in α of 0.1, 0.2 and 1% at $\theta = 89.0$, 89.5 and 89.95°, respectively. The absolute value of this error is not sensitive to α values; this means that, for small α values as in the case of silicon, the effect can be more serious in particular at a higher θ. In other words, the number of significant figures of the α value that can be obtained by U-HADOX may be four at most. In addition, the error is in proportion to the spacing; the measurement for larger hkl's is therefore advantageous also from this point of view.

By the use of synchrotron X-rays, most of the difficulties so far mentioned will disappear or be reduced. First, one may use a diffractometer with the distance between two crystals 10 m or longer. This guarantees the measurement at $\theta = 89.95^\circ$. Second, the detector can be used at the position shown in Fig. 3 of OS, where the detector receives both the incident and diffracted beams; as described by Shvyd'ko & Gerdau (1999), we can separately observe these beams on the time-resolved spectrum. The Bond method, which needs monochromatic X-rays, is no longer necessary to determine the position of $\theta = 90^\circ$, because one can attain enough accuracy by measuring the separation between the incident and diffracted beams (*cf.* §3).

U-HADOX will be especially useful if the linear thermal-expansion coefficient is too small to be measured by conventional X-ray diffraction. This means that U-HADOX is generally useful at low temperatures. An extreme example is the anomaly in the lattice constant in silicon, germanium, gallium arsenide *etc.* with the diamond or zinc-blende type of structure. In each case, the thermal-expansion coefficient

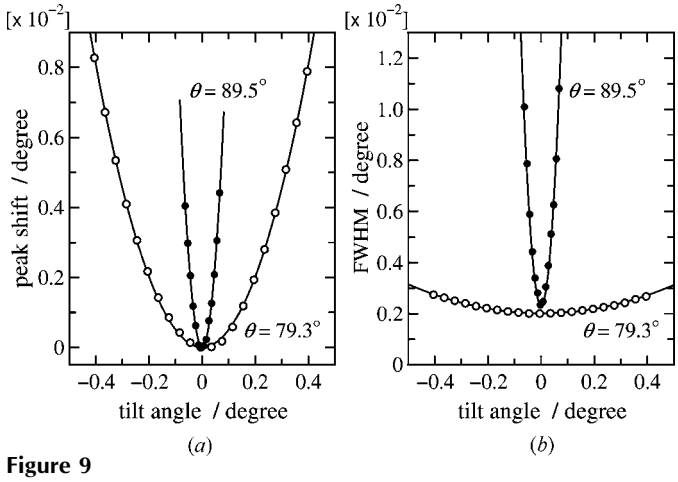

Figure 9
Effect of the crystal tilt on the peak shift (*a*) and on the width (FWHM) (*b*) of hhh of silicon in HADOX measurements. Curves are quadratic functions of the tilt that are fitted to the data.

changes the sign from plus to minus with decreasing temperature; this occurs in silicon, for example, around 120 K. U-HADOX will be suitable to investigate the physics involved in such anomalies.

In semiconductor technology, the matching of the lattice spacing between a thin-film crystal and a substrate on which the crystal is grown is an important parameter. In future, as a consequence of advanced precision, the matching of thermal expansivity might also be taken into account; U-HADOX would be useful for characterization in such cases.

7. Conclusions

The performance of HADOX has been upgraded at ultra-high Bragg angles. From the data of U-HADOX on silicon at $\theta = 89.5^\circ$, it is concluded that the relative accuracy of a change in the lattice spacing is 10^{-8}, and can be improved to 10^{-9} at $\theta = 89.95^\circ$. The linear thermal-expansion coefficient of silicon around 300 K has been determined with four significant figures by varying the temperature by 1 K; the sensitivity is higher than that attained by the macroscopic thermal-expansion experiments (Bergamin *et al.*, 1997; Lyon *et al.*, 1977; Norton *et al.*, 1976). By using synchrotron X-rays, even higher accuracy will be attained. The best performance of U-HADOX will be realized by measuring diffraction at highest θ for large *hkl*'s; such a combination guarantees the highest sensitivity for the peak shift as well as the highest resolution owing to the smallest $F(hkl)$ and λ giving the smallest FWHM of the peak. It should be emphasized that the method is also applicable to less perfect crystals.

In a moderately high angle range of θ, *e.g.* 80–85°, the accuracy will also be moderate, being one or two orders of magnitude lower; neither the effect of a mismatch of the lattice spacing of coupled crystals nor the effect of temperature fluctuation can be very serious then. This will make the experiment much easier.

Note added in proof: The authors appreciate the comment, given by Professor A. Authier at the XIX Conference on Applied Crystallography, held September 2003 in Kraków, Poland, that the dynamical theory is not applicable at $\theta = 90^\circ$.

The authors are grateful to Professor Y. Soejima for support and discussions, and to Professor H. Sakashita for use of the facility at the Centre of Advanced Analysis, Kyushu University. Thanks are also due to Shin-Etsu Handotai Co. Ltd and Dr H. Hünnefeld, Hasylab at DESY, for offering single crystals of silicon and of $SrTiO_3$, respectively. One of the authors (AO) appreciates discussions with Mr S. Nagao and Dr A. Kohno. Introduction of the reference Watanabe *et al.* (2002) and the related papers by one of the referees is also appreciated.

References

Bartels, W. J. (1983). *J. Vac. Sci. Technol.* B**1**, 338–345.
Batchelder, D. N. & Simmons, R. O. (1964). *J. Chem. Phys.* **41**, 2324–2329.
Bednorz, J. G. & Scheel, H. J. (1977). *J. Cryst. Growth*, **41**, 5–12.
Bergamin, A., Cavagnero, G. & Mana, G. (1997). *J. Appl. Phys.* **82**, 5396–5400.
Bond, W. L. (1960). *Acta Cryst.* **13**, 814–818.
Lu, Z., Munakata, K., Kohno, A., Soejima, Y. & Okazaki, A. (1995). *Mater. Sci. Eng.* B**34**, 220–223.
Lyon, K. G., Salinger, G. L., Swenson, C. A. & White, G. K. (1977). *J. Appl. Phys.* **48**, 865–868.
Norton, M. A., Berthold, J. W. III, Jacobs, S. F. & Plummer, W. A. (1976). *J. Appl. Phys.* **47**, 1683–1685.
Okada, Y. & Tokumaru, Y. (1984). *J. Appl. Phys.* **56**, 314–320.
Okazaki, A. & Kawaminami, M. (1974). *Ferroelectrics*, **7**, 91–92.
Okazaki, A. & Ohama, N. (1979). *J. Appl. Cryst.* **12**, 450–454.
Okazaki, A. & Soejima, Y. (2001). *Acta Cryst.* A**57**, 708–712.
Shvyd'ko, Y. V. & Gerdau, E. (1999). *Hyperfine Interactions*, **123/124**, 741–776.
Watanabe, H., Yamada, N. & Okaji, M. (2002). *Int. J. Thermophys.* **23**, 543–554.